



Progress in Ti_3O_5 : Synthesis, properties and applications

Peng-fei ZHAO^{1,2*}, Guang-shi LI^{1,2*}, Wen-li LI^{1,2}, Peng CHENG^{1,2},
Zhong-ya PANG^{1,2}, Xiao-lu XIONG^{1,2}, Xing-li ZOU^{1,2}, Qian XU^{1,2}, Xiong-gang LU^{1,2,3}

1. School of Materials Science and Engineering, Shanghai University, Shanghai 200444, China;
2. State Key Laboratory of Advanced Special Steel & Shanghai Key Laboratory of Advanced Ferrometallurgy, Shanghai University, Shanghai 200444, China;
3. School of Materials Science, Shanghai Dianji University, Shanghai 201306, China

Received 18 October 2021; accepted 18 November 2021

Abstract: The crystal structure, physical, chemical and phase transition properties of trititanium pentoxide (Ti_3O_5) have aroused a broad range of research effort since the 1950s. Different crystalline forms (α , β , γ , δ and λ) of Ti_3O_5 exhibit various properties. Particularly, reversible phase transitions between λ - and β - Ti_3O_5 have been attracting increasing research interest, which brings new potential applications of Ti_3O_5 materials in the field of energy and data storage. More recently, Ti_3O_5 materials have shown excellent performance in trace detection, microwave absorption and virus adsorption, which has expanded its application fields. Here, the essential properties of different crystal forms of Ti_3O_5 are described in detail. An intensive overview of Ti_3O_5 preparation methods and applications is comprehensively summarized.

Key words: Ti_3O_5 ; phase transition; pressure induction; data storage; catalyst support

1 Introduction

Aside from stoichiometric titanium dioxide (TiO_2), which has been studied extensively and used in numerous fields ranging from alloys to photo-catalytic materials, titanium binary oxides have a series of suboxides. These titanium suboxides comply with the generic formula of Ti_nO_{2n-1} and include NaCl-type TiO , corundum-type Ti_2O_3 and “Magnéli phases” Ti_nO_{2n-1} ($n \geq 3$) [1–12]. However, whether trititanium pentoxide (Ti_3O_5) belongs to this series remains controversial because the typical shear planes existing in Magnéli phases are not found in the crystal structure [13–15].

Since the 1950s, many scholars have conducted considerable research on Ti_3O_5 . Yet, the focus is mostly on structure, physical and chemical properties, and five different Ti_3O_5 crystal structures (α , β , γ , δ and λ) have been identified [16]. These phases are closely related structurally and exhibit different properties in terms of conductivity, magnetism and electronic structure. In addition, there are some intriguing phase-transition characteristics between them under different external conditions. At room temperature, bulk Ti_3O_5 is kept in the form of a stable β phase with a monoclinic structure. However, this phase transforms into the λ phase at 460 K with an isostructural phase transition and further transforms into the α phase at 514 K, undergoing a structural

Corresponding author: Guang-shi LI, Tel: +86-21-66136518, E-mail: lgs@shu.edu.cn;
Xiao-lu XIONG, Tel: +86-21-66136518, E-mail: xlxiong@t.shu.edu.cn;
Xing-li ZOU, Tel: +86-21-66136518, E-mail: xlzou@shu.edu.cn

*Peng-fei ZHAO and Guang-shi LI contributed equally to this work

DOI: 10.1016/S1003-6326(21)65731-X

1003-6326/© 2021 The Nonferrous Metals Society of China. Published by Elsevier Ltd & Science Press

transition from monoclinic to orthorhombic. γ - Ti_3O_5 can be obtained through slow cooling of α - Ti_3O_5 at high temperatures, transforming into δ - Ti_3O_5 at approximately 237 K.

Recently, the research on Ti_3O_5 has mainly focused on its preparation methods and applications as functional materials, as shown in Fig. 1. In 2003, the first applications of Ti_3O_5 for oxygen sensors were reported. The features of metal-like and variable atom ratio of oxygen to titanium confer α - Ti_3O_5 potential applications in oxygen sensors. TiO_2 is a widely studied photo-catalytic material, and titanium suboxides, such as Ti_2O_3 , Ti_4O_7 and Ti_8O_{15} , also exhibit good photo-activity due to the existence of oxygen vacancies. Therefore, the photo-catalytic activity and performance of Ti_3O_5 have also been studied. Furthermore, Ti_3O_5 holds the advantages of good chemical stability, non-toxicity and good acid and alkali resistance through which it can be recommended for catalyst support applications. In addition, the discovery of the photo-induced phase transition between λ and β phases has raised a new discussion and piqued research interest in science, introducing new applications into optical memory. This intriguing reversible phase transition could also be triggered by other external stimulation, such as pressure, temperature and current, which further broadened

the application of Ti_3O_5 in energy storage, THz sensors and smart windows [17]. Recently, the excellent performance of Ti_3O_5 in trace detection, microwave absorption and virus adsorption has provided broad prospects for its future application.

Although there are intensive experimental and computational studies, a comprehensive summary of the structure, physical properties, preparation and application of Ti_3O_5 is lacking. A deep understanding of the basic physicochemical properties of Ti_3O_5 might aid in developing applications in new areas. As a result, we initially discussed synthetic approaches of Ti_3O_5 . Especially, we systematically discussed crystal and chemical structure properties of different crystal forms of Ti_3O_5 , including reversible phase transition phenomena between them. Through this discussion, we summarized a comprehensive overview of the application of Ti_3O_5 in gas sensors, energy storage, optical storage media, catalysts and other new application fields. Finally, the focus for the future direction of Ti_3O_5 was provided.

2 Synthetic approaches for trititanium pentoxide (Ti_3O_5)

Numerous methods have been reported for preparing Ti_3O_5 since it was identified. Typically,

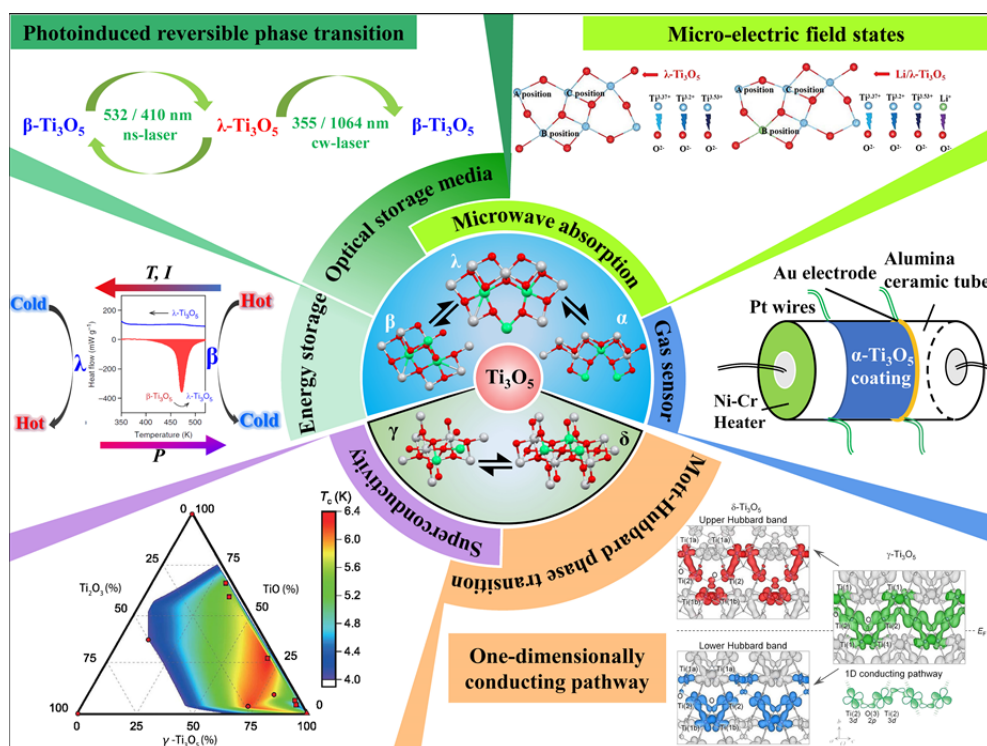
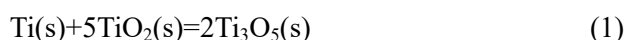


Fig. 1 Schematic of application of different crystal forms of trititanium pentoxide (Ti_3O_5) in various fields

TiO₂ is selected as the raw material for preparing Ti₃O₅ by using reduction methods, and metal titanium, carbon, carbonaceous organic material or reducing atmosphere (H₂, CO) can be used as reducing agents for preparing Ti₃O₅ using reduction methods. Reducing agents, which have a higher oxygen affinity, are oxidized to their corresponding oxides, reducing TiO₂ to Ti₃O₅, simultaneously. In addition, some methods such as electro-chemical reduction and pulsed laser deposition (PLD) are also used to meet the need to obtain different forms or properties of Ti₃O₅.

2.1 Metallothermic reduction

Metal titanium is the most commonly used reductant at the start of the preparation of Ti₃O₅. The key to preparing a high purity target product lies in the appropriate ratio of titanium to TiO₂. The reduction processes work at temperatures above 1000 °C under an inert atmosphere for several days using an electric arc furnace or electric resistance furnace, as shown in Fig. 2. The redox reaction is given as follows:



For instance, in the experiments of ÅSBRINK and MAGNÉLI [18], TiO₂ and Ti were used as raw materials and mixed with a stoichiometric ratio to prepare Ti₃O₅ using an electric arc furnace under an argon atmosphere. After two-week annealing at 1150 °C, high-quality β-Ti₃O₅ was obtained. To prepare γ-Ti₃O₅ films, KUROKAWA et al [19] firstly synthesized Ti₂O₃ by sintering mixed Ti and TiO₂ pellets at 1000 °C for 12 h. Secondly, γ-Ti₃O₅ films grew on α-Al₂O₃ (0001) substrates using Ti₂O₃ as a target by the PLD method. Using the same method, FAN et al [20] used titanium metal as a target to directly grow γ-Ti₃O₅ on α-Al₂O₃ (0001) substrates by tuning the oxygen pressure. In contrast to other reported targets, titanium has the advantage of easily preparing Ti₃O₅ films because this is an exothermic process and the oxygen content is easy to control. Titanium is an ideal

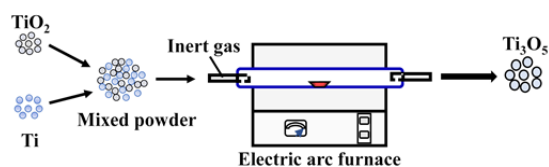


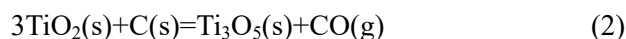
Fig. 2 Schematic illustration of metallothermic reduction process

reductant because no impurities are introduced in this process. However, this method is limited by high costs and prolonged treatment time.

In addition, KITADA et al [21] selected Zr as a reductant and TiO₂ as a titanium source using the sol-gel method to prepare macroporous titanium suboxides (Ti_nO_{2n-1}; n=2, 3, 4, 6). Firstly, porous TiO₂ precursor monolith was fabricated using ethyl acetoacetate as a chelating agent and NH₄NO₃ as mineral salt. Then, several suboxides were obtained under different reduction degrees depending on the amount of the reductant. A single phase of Ti₃O₅ can be prepared under a 6:1.05 molar ratio of TiO₂ to Zr at 1150 °C. The as-prepared Ti₃O₅ had a macroporous structure with low bulk densities (1.78 g/cm³) and large porosities (58%).

2.2 Carbothermal reduction

To develop an efficient, economical and rapid method for preparing nano-λ-Ti₃O₅, CHAI et al [22] proposed a carbothermal reduction method. The redox reaction is given as follows:



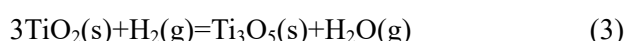
The key to preparing a high purity target product lies in the appropriate ratio of carbon to TiO₂. In addition, the roasting temperature, holding time and argon gas flow rate were also studied in detail. λ-Ti₃O₅ was synthesized at 1050 °C under 4.5 wt.% carbon black content for 3 h in an inert atmosphere. The resulting powder had a specific surface area of 12.82 m²/g with an average particle size of (3.0±1.0) μm. After that, using the same reduction approach, they reported the effect of coating layers, such as Al₂O₃ or SiO₂, on the formation of nano-λ-Ti₃O₅. In 2020, a new approach using commercial polyethylene glycol 600 as a carbon source and tetra-*n*-butyl titanate as a titanium source was reported by CAI et al [23]. Spherical shape powder with an average particle size of 40 nm was obtained at 1070 °C for 2 h. Subsequently, YANG et al [24] were inspired by the preparation of Ti_nO_{2n-1} using polyvinyl alcohol as a carbon source and proposed using phenol resin, which had highly reduced properties, as reducing agents to prepare recorded purity β-Ti₃O₅ compacts. The β-Ti₃O₅ of the final product was as high as 98.06% according to X-ray diffraction (XRD) refinement results.

The carbothermal reduction has unique

advantages such as high yield and economic and environmental friendliness; however, it is difficult to avoid carbon residue within the as-prepared Ti_3O_5 .

2.3 Hydrogen reduction

In 1968, IWASAKI et al [25] used TiO_2 as a titanium source and H_2 as a reductant to synthesize Ti_3O_5 . A D-type phase, hereafter called λ - Ti_3O_5 , was obtained at 1250 °C for 3 h in a hydrogen gas stream. The redox reaction is given as follows:



To prepare α - Ti_3O_5 thin films, ZHENG [26] used $\text{Ti}(\text{OC}_4\text{H}_9)$ as a titanium resource to obtain Ti^{4+} containing sol. Firstly, TiO_2 thin films were fabricated by a dip-coating method on Al_2O_3 substrates. Secondly, after reducing these TiO_2 thin films with hydrogen at 1200 °C for 4 h, α - Ti_3O_5 thin films were formed. To prepare nano- λ - Ti_3O_5 , OHKOSHI et al [27] selected TiO_2 as raw material and reduced it under hydrogen stream (0.3 dm^3/min) at 1200 °C for 2 h. The prepared crystals were composed of nano-crystals in (25±15) nm with a flake form. In addition, a combination of reverse-micelle and sol-gel method was also used to synthesize nano- λ - Ti_3O_5 . The process is illustrated in Fig. 3 [28], and the prepared sample has a cubic shape with (21±11) nm. Using this approach, NASU et al [28] synthesized different grain sizes of λ - Ti_3O_5 by controlling the sintering temperature; however, the hydrogen flow rate did not influence it.

In the experiments of ALIPOUR MOGHADAM ESFAHANI et al [29], to obtain catalyst support that contains Ti_3O_5 , TiO_2 was selected as a titanium source and a gaseous mixture containing hydrogen ($\text{H}_2:\text{N}_2$ 10:90, vol.%) as a reducing agent.

The problems of carbon residue and other impurities can be solved well; however, the potential explosion hazard restricts its applications.

2.4 Carbon monoxide reduction

In addition to hydrogen reduction, crystal growth under CO reducing atmosphere is also a practical method for preparing Ti_3O_5 in the early years. For instance, BARTHOLOMEW and WHITE [30] successfully grew Ti_3O_5 from $\text{Na}_2\text{B}_4\text{O}_7$ - B_2O_3 flux by controlling oxygen fugacity under the CO atmosphere, which originated from graphite. The Ti_3O_5 single crystal was obtained under a certain oxygen fugacity at 1300 °C.

2.5 Electro-chemical reduction

Since the electro-chemical de-oxidization of TiO_2 in molten calcium chloride to directly prepare titanium was proposed by CHEN et al [31] many scholars have dedicated effort to the in-depth study of this process [31,32]. DRING et al [33] investigated cathodic de-oxygenation of TiO_2 at 900 °C under certain potentials lower than those of the formation of calcium. The reduction from TiO_2 to Ti_3O_5 was detected at a potential of 300 mV, which was negative for the TiO_2 open-circuit on the TiO_2 working electrode. Further studies on pre-dominance diagrams were also conducted by them to better understand the electro-chemical de-oxidization of TiO_2 [34]. On this basis, the kinetic parameters related to different reduction processes were calculated by KAR and EVANS [35] using a coupled electro-chemical and diffusion model. These studies have demonstrated the feasibility and availability of the proposed approach; however, they mainly focused on electro-chemical de-oxidization processes of TiO_2 rather than the preparation of Ti_3O_5 . After that, ERTEKIN et al [36] developed a one-step electro-deposition method for synthesizing $\text{Ti}_n\text{O}_{2n-1}$ films by an electro-deposition method using an acetonitrile solution as a supporting electrolyte. TiOSO_4 and H_2O_2 play a major role in this process, and both γ - Ti_3O_5 and λ - Ti_3O_5 can be obtained from indium-tin-oxide coated glass substrates at certain potentials and

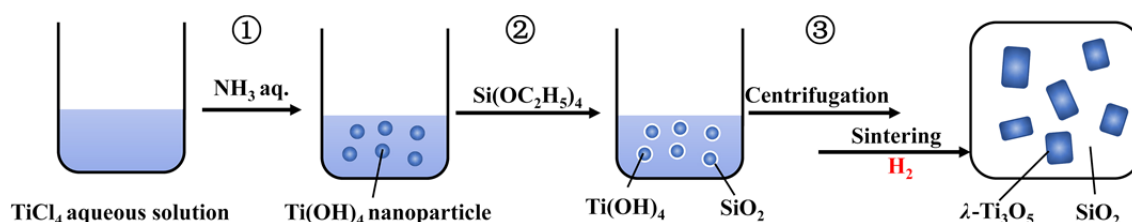


Fig. 3 Schematic of λ - Ti_3O_5 nano-crystal synthesis process [28]. Reproduced with permission. Copyright 2014, Institute of Physics Publishing

temperatures. In their follow-up work, β - Ti_3O_5 was also detected on the substrates using the same methods [37]. These studies provided a new idea for preparing Ti_3O_5 thin films with the advantage of without requiring additional heating. However, the obtained products are a complex mixture of titanium sub-oxides or a mixture of Ti_3O_5 with different crystals. Therefore, further optimization regarding deposition conditions is needed.

2.6 Chemical vapor transport

In addition, a cheaper, efficient and easy method called chemical vapour transport was applied to the crystal growth of Ti_2O_3 [38]. After that, a series of titanium suboxide crystals were fabricated using this method. MERCIER et al [39] selected TiO_2 as the starting material and used hydrogen to reduce it to the desired suboxide. Then, they selected TeCl_4 or NH_4Cl as a transport agent for the single-phase growth of Ti_3O_5 . STROBEL and PAGE [40] used TeCl_4 or Cl_2 as a transport agent to prepare $\text{Ti}_n\text{O}_{2n-1}$ with $n=2-9$. Most of the samples were twinned crystals because of the particular sensitivity of Ti_3O_5 to oxygen. In experiments of HONG [41], commercial TiO_2 and titanium were used as raw materials, and they were mixed at a suitable stoichiometric ratio. The mixed powders were annealed in an arc furnace under an argon atmosphere to obtain Ti_2O_3 and β - Ti_3O_5 , which were mixed in stoichiometric proportions. Then, the obtained mixtures were pressed into pellets, which were used to prepare single crystals of γ - Ti_3O_5 using TiCl_4 as a transport agent. Notably, this is the first report on the preparation of single crystals of γ - Ti_3O_5 . After that, the crystal structure and physical properties of γ - Ti_3O_5 were studied systematically by HONG and ÅSBRINK [42].

3 Structures and properties

3.1 Phase structures

Ti_3O_5 is a polycrystalline compound with variable crystallographic structures (β , λ , α , γ and δ). The schematic representation and lattice parameters of the different crystal structures are shown in Fig. 4 and Table 1 (β phase: ICSD card No. 75194; λ phase: ICSD card No. 75193; α phase: ICSD card No. 50984; γ phase: ICSD card No. 35148; δ phase: CCDC card No. 1004604).

β - Ti_3O_5 , originally known as the LM (low-temperature) structure, is a stable phase at room temperature with a monoclinic symmetry and space group $C2/m$. Figure 4(a) shows that there are three independent Ti atomic sites, labelled Ti(1), Ti(2) and Ti(3), respectively and each of them is octahedrally coordinated to six oxygen atoms, forming a distorted TiO_6 structure. The crystal could be viewed as comprising TiO_6 by sharing corners on the b -axis and edges in the ac plane. The average valences for Ti(1), Ti(2) and Ti(3) are 3.0, 3.7 and 3.3, respectively [43]. λ - Ti_3O_5 , originally known as the HM (high-temperature) structure, is a meta-stable phase with monoclinic symmetry and space group $C2/m$. As shown in Fig. 4(b), distorted TiO_6 shares six edges with its neighbours. This specialised junction makes Ti atoms with the same atomic environment, and the average valence is 3.3. α - Ti_3O_5 , hereafter called the HO (high temperature orthorhombic) structure, with orthorhombic symmetry and space group $Cmcm$ is a high-temperature phase [44]. Figure 4(c) shows that the crystal could be viewed as comprising TiO_6 by sharing corners on an axis and sharing six edges with its neighbours. There are two independent Ti atomic sites, labelled Ti(1) and Ti(2), respectively and their average valence is 3.3. γ - Ti_3O_5 , which is another stable phase at room temperature with monoclinic symmetry and space group $I2/c$. It was reported by ÅSBRINK et al [45], and the structure is shown in Fig. 4(d). There are two independent Ti atomic sites, labelled Ti(1) and Ti(2), respectively and the crystal structure could be viewed as comprising two characteristic chains. One chain is made of regular Ti(1)O_6 octahedra joined by shared corners, whereas the other one has distorted Ti(2)O_6 octahedra joined by shared edges and a common face. The valence states for Ti(1) and Ti(2) are 3.36 and 3.30, respectively. In δ - Ti_3O_5 (Fig. 4(e)), the Ti(1) site of γ - Ti_3O_5 becomes two different sites, labelling Ti(1a) and Ti(1b), respectively, thereby forming three independent Ti atomic sites, with corresponding valence states of 3.66, 3.16 and 3.2, respectively [46].

3.2 Phase transition properties

Phase transitions between Ti_3O_5 phases have been identified in numerous studies. These phases experience different transition processes during

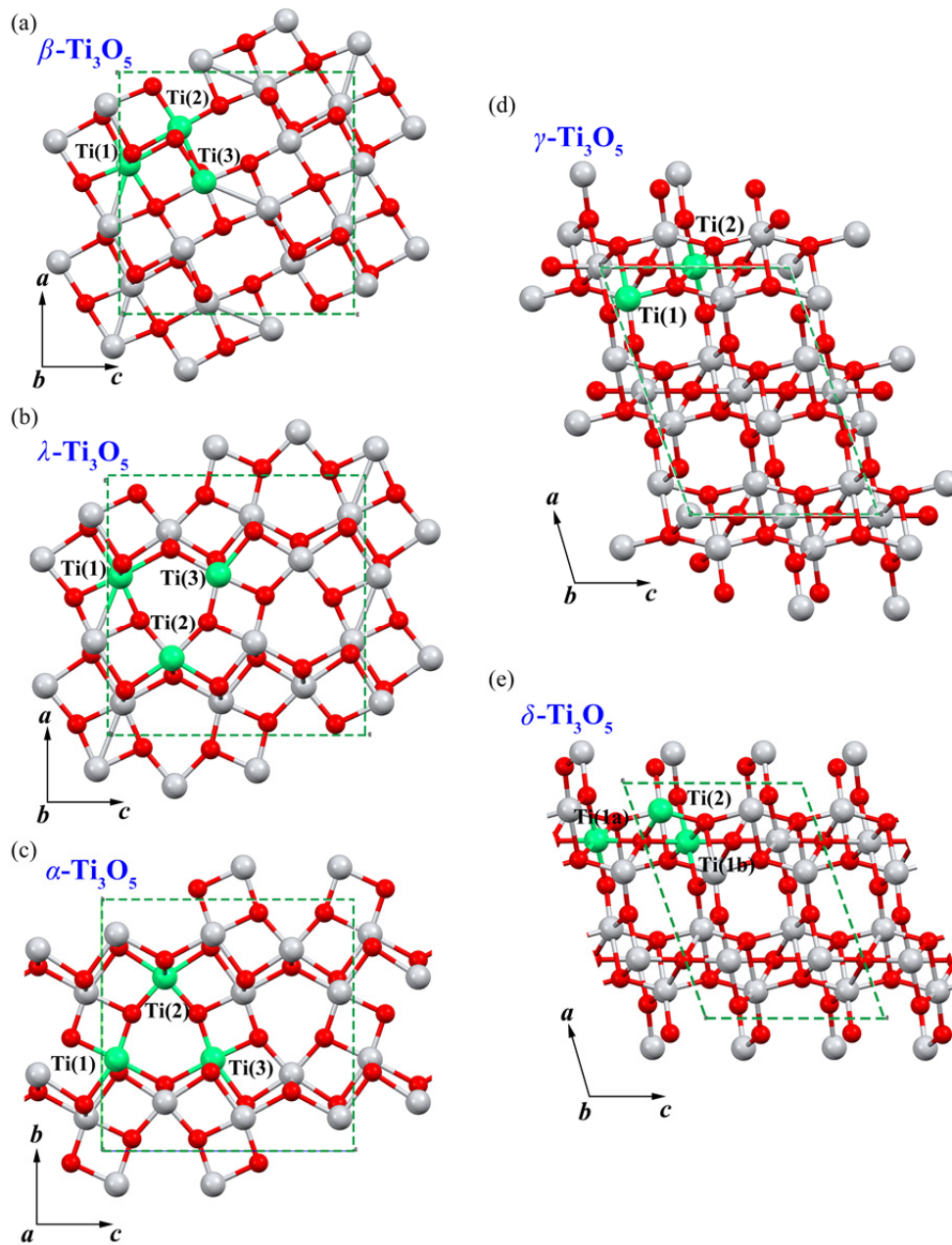


Fig. 4 Schematics of crystal structures of Ti_3O_5 (β , λ , α , γ and δ)

Table 1 Lattice parameters of different Ti_3O_5 phases

Phase	Crystal system	Space group	$a/\text{\AA}$	$b/\text{\AA}$	$c/\text{\AA}$	$\beta/(\text{^\circ})$	$V/\text{\AA}^3$
$\beta\text{-Ti}_3\text{O}_5$	Monoclinic	$C2/m$	9.7568 (2)	3.80077 (9)	9.4389 (1)	91.547 (1)	349.9
$\lambda\text{-Ti}_3\text{O}_5$	Monoclinic	$C2/m$	9.8261 (2)	3.78937 (9)	9.9694 (2)	91.258 (2)	371.12
$\alpha\text{-Ti}_3\text{O}_5$	Orthorhombic	$Cmcm$	3.798 (2)	9.846 (3)	9.988 (4)	90	373.5
$\gamma\text{-Ti}_3\text{O}_5$	Monoclinic	$I2/c$	9.9701 (5)	5.0747(3)	7.1810(4)	109.865(4)	341.71
$\delta\text{-Ti}_3\text{O}_5$	Monoclinic	$P2/a$	9.9651(7)	5.0604(4)	7.2114(5)	109.3324(9)	343.15(4)

warming and cooling with corresponding changes in lattice parameters, magnetic state and electric resistivity. During the heating process, the

room-temperature stable β phase transforms into a meta-stable λ phase at approximately 460 K with the first-order phase transition and an abrupt

reduction of resistivity from semiconductors to metals [47,48]. The lattice parameters are also changed, especially the expansion of the c -axis, increasing the volume. As the temperature is increased to 514 K, the λ phase further transforms into the α phase with the second-order phase transition [49]. However, there is no sudden change in the magnetic state and resistivity. The meta-stable λ phases can be stabilized at room temperature by introducing impurity elements such as Fe, V, Mg, Li and Al, and with an increase in impurity content, the transition temperature is decreased accordingly [50–55]. In addition, the meta-stable λ phase could also be stabilized at room temperature in nano-scale, exhibiting a reversible phase transition between λ and β by an external stimulus such as laser light, pressure, temperature and current [56].

During the cooling process, the room-temperature stable γ phase transforms into the δ phase at approximately 237 K, which undergoes a Mott–Hubbard metal-insulator phase transition due to the breaking of a one-dimensionally conducting pathway, as shown in Fig. 5 [46]. From the electrical conductivity and optical measurement results, the γ phase has metallic conductor properties, whereas the δ phase exhibits semiconductor properties, as shown in Fig. 5(b). However, different results were obtained in terms of

phase-transition temperature (225 K) in the thin film of the γ phase [57]. The most likely reason would be internal stress or strain caused by lattice-constant mismatches and different expansion coefficients between the substrate and product.

4 Applications of trititanium pentoxide (Ti_3O_5)

4.1 Gas sensor

Ti_3O_5 is considered the most promising gas sensor substitute in high-temperature solid-state gas sensors. ZHENG [58] used α - Ti_3O_5 in oxygen sensing for the first time. α - Ti_3O_5 thin films were synthesized by hydrogen reduction TiO_2 thin films, which were obtained on Al_2O_3 substrates using $\text{Ti}(\text{OC}_4\text{H}_9)_4$ as a precursor. The α - Ti_3O_5 thin films exhibited an impressive low resistivity–temperature coefficient with better high-temperature stability and reproducibility. However, their oxygen sensitivity needs to be further improved. After that, significant improvements in oxygen sensitivity and response rate were achieved by 5 at.% Ce and 1 at.% W doping, which offer more effective active sites on the surface of materials [26]. Compared with pure α - Ti_3O_5 , W doping reduced the resistivity–temperature coefficient, whereas Ce doping increased the structure stable temperature to 700 °C. ZHANG et al [59] synthesized Ti_3O_5 sub-micron

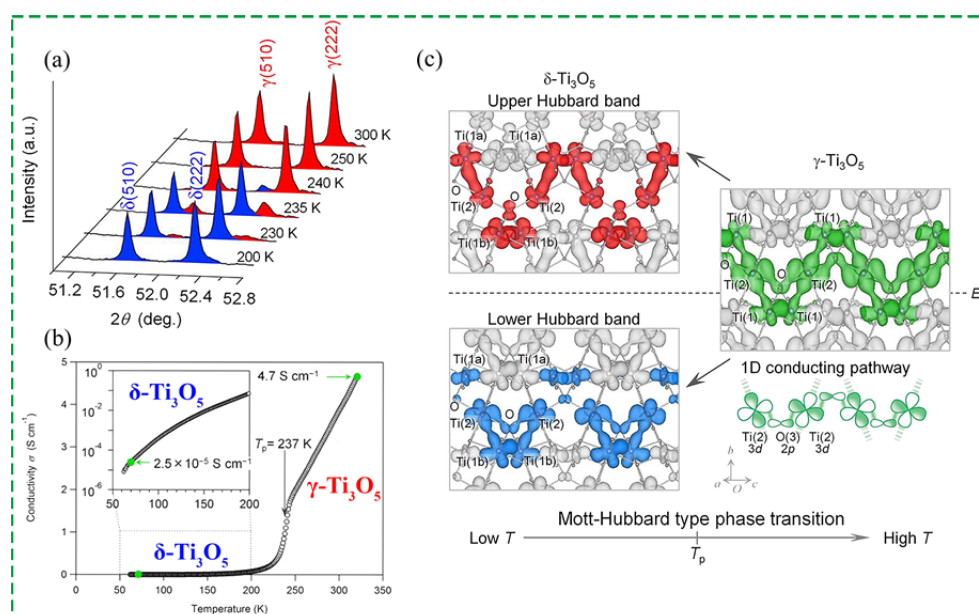


Fig. 5 Phase transition mechanism: (a) X-ray diffraction patterns of phase transition between γ - and δ - Ti_3O_5 with temperature; (b) Temperature dependence of electrical conductivity; (c) Charge density maps for transformation from γ to δ phases [46]. Reproduced with permission. Copyright 2015, American Chemical Society

rods by a sintering method using H_3TiO_5 nano-fibers as a precursor. However, the sensor characteristics are not satisfactory.

LI et al [60] prepared $\beta\text{-Ti}_3\text{O}_5$ by carbothermal reduction of TiO_2 , demonstrating certain oxygen sensitivity by experiment and density functional theory (DFT) calculations. However, its performance is not good based on the response and recovery time in 20% O_2 +80% N_2 and 20% H_2 +80% N_2 atmospheres. Therefore, further optimization is required.

4.2 Energy storage material

$\lambda\text{-Ti}_3\text{O}_5$ is a meta-stable phase and frequently appears at high temperatures. OHKOSHI et al [27,56] found that $\lambda\text{-Ti}_3\text{O}_5$ could exist at room temperature with nano-scale ((25±15) nm or (21±11) nm) due to thermodynamic local energy minimum. The as-prepared nano- $\lambda\text{-Ti}_3\text{O}_5$ was a metallic conductor and showed Pauli paramagnet. In addition, they found a reversible phase transition phenomenon between λ and β phases. It can be induced by laser light, which confers enormous potential in optical storage media. Subsequently, TOKORO et al [61] reported other induced reversible phase-transition factors, such as pressure, temperature and current, and specifically, $\lambda\text{-Ti}_3\text{O}_5$ could transform into $\beta\text{-Ti}_3\text{O}_5$ under external pressure with heat release. Vice versa, $\beta\text{-Ti}_3\text{O}_5$ could absorb heat from the external environment, transforming it into $\lambda\text{-Ti}_3\text{O}_5$ under external stimuli such as heat, current and light. This feature gives Ti_3O_5 enormous potential in heat storage. The absorbed energy during the phase transition from β to λ was (230±20) kJ/L with an induced temperature, and (240±40) kJ/L energy was released from λ to β with an induced pressure.

Because $\lambda\text{-Ti}_3\text{O}_5$ can only exist at room temperature with nano-scale, WEI et al [62] studied the effect of coating layers on the stability of meta-stable phase $\lambda\text{-Ti}_3\text{O}_5$. In their experiment, inorganic layers, such as Al_2O_3 or SiO_2 , were coated on the nano-rutile TiO_2 particles to prepare $\lambda\text{-Ti}_3\text{O}_5$. Results indicated that the $\text{Al}_2\text{O}_3\text{-SiO}_2$ dual-coated TiO_2 sample emerged as $\lambda\text{-Ti}_3\text{O}_5$. However, a similar phenomenon was not found in the uncoated or SiO_2 -coated TiO_2 sample. Therefore, the introduction of Al^{3+} from the coating layer played an important role in the formation and stabilization of $\lambda\text{-Ti}_3\text{O}_5$. After that, they proposed a

doping strategy to investigate the stabilizing effect of Al^{3+} on $\lambda\text{-Ti}_3\text{O}_5$ [63]. From the d-spacing of the (110) plane, the value of the Al^{3+} doped sample (0.35 nm) was lower than the typical value (0.37 nm), indicating that Al^{3+} was doped in the substitutional mode. The as-prepared samples could exist at room temperature with a micro-crystal scale (2 μm) under 6.0 at.% Al doping. Furthermore, the effect of Al^{3+} doping on phase transition was extensively investigated. The results indicated that Al^{3+} doping not only reduced the transition temperature ($\beta \rightarrow \lambda$) but also promoted the transition from β to λ . In 2019, WANG et al [64], inspired by the reference to the MgO-TiO_2 equilibrium phase diagram, proposed an Mg doping strategy to stabilize $\lambda\text{-Ti}_3\text{O}_5$ at room temperature. Similar results concerning phase-transition properties were obtained. Note that the stabilization effects of Mg doping were more efficient than those of Al doping in terms of requiring less amount of Al^{3+} . A possible reason was the larger ionic radius and lower valence of Mg^{2+} .

In 2019, OHKOSHI et al [65] prepared a heat storage ceramic and used it to recycle waste heat from automobiles. The grain size of as-prepared $\lambda\text{-Ti}_3\text{O}_5$ was 10 times larger than that of previous samples of hydrogen reduction, called block-type $\lambda\text{-Ti}_3\text{O}_5$. From pressure-induced results, the phase transition from λ to β required a relatively low external pressure (50% transforms under 7 MPa). Temperature-induced results showed that the endothermic peak was at approximately 471 K (198 °C) with 237 kJ/L. After that, inspired by the aforementioned metal doping strategy, NAKAMURA et al [66] calculated the formation energy of $\lambda\text{-Ti}_3\text{O}_5$ with 54 different doping elements, and the results indicated that only six elements (Sc, Zr, Nb, Hf, Ta and W) promoted the formation of the λ phase with lower formation energy. Subsequently, bulk Ti_3O_5 was prepared using TiO_2 as a titanium source and Ti as a reductant with different doping elements by an arc-melting technique, as shown in Fig. 6 [66]. However, only Sc doping formed the λ phase according to the XRD result. Sc doping content materials were synthesized, and the chemical formulas were $\text{Sc}_{0.09}\text{Ti}_{2.91}\text{O}_5$, $\text{Sc}_{0.105}\text{Ti}_{2.895}\text{O}_5$ and $\text{Sc}_{0.108}\text{Ti}_{2.92}\text{O}_5$. Temperature-induced results showed that the corresponding endothermic peaks were at about 67, 45 and 38 °C, respectively. Compared with

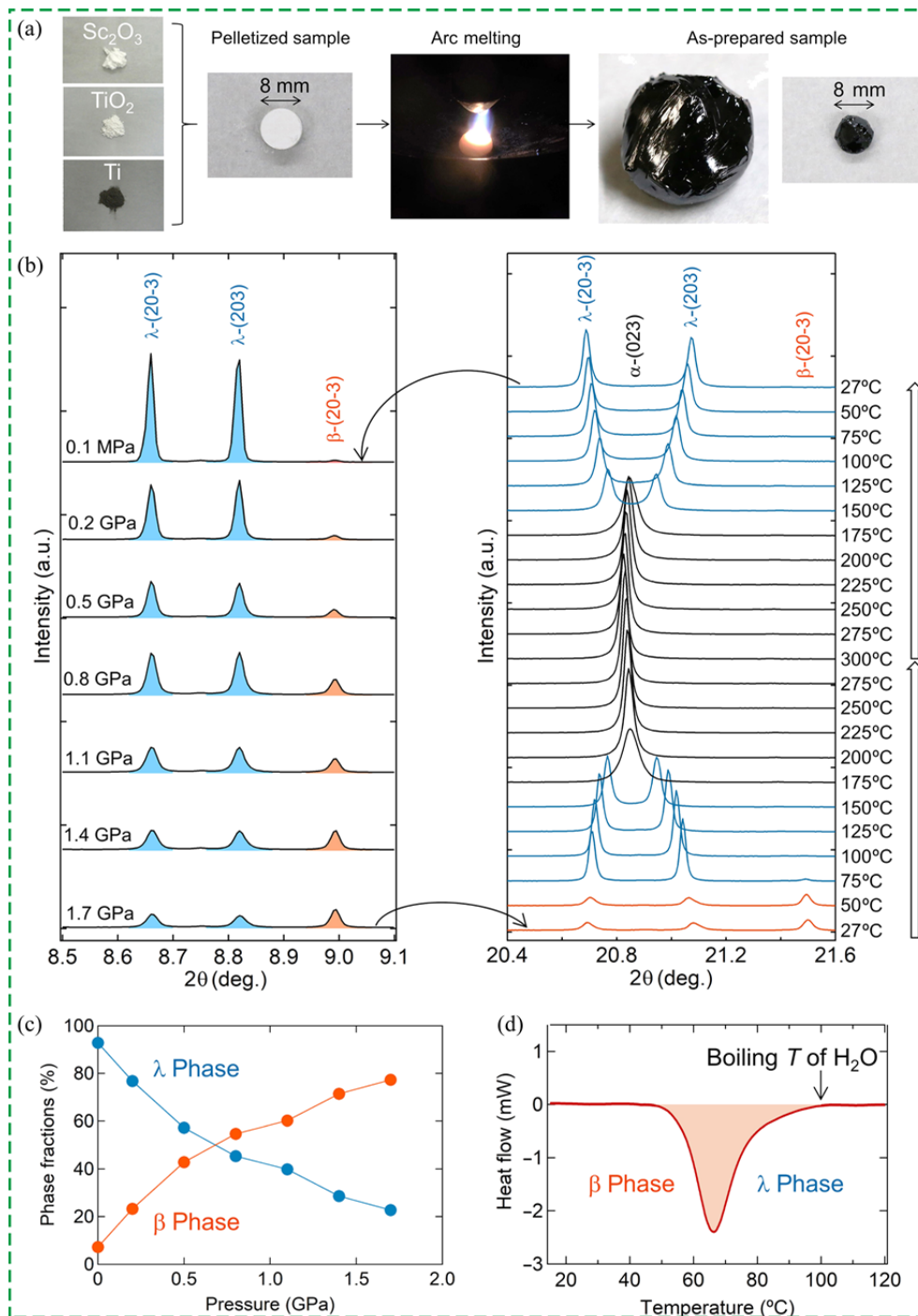


Fig. 6 (a) Schematic of synthetic process of bulk λ - $\text{Sc}_{0.09}\text{Ti}_{2.91}\text{O}_5$; (b) Synchrotron X-ray diffraction patterns of pressure and temperature-induced phase-transition process; (c) Phase fractions at different pressures; (d) Endothermic performance from β to λ [66]. Reproduced with permission. Copyright 2020, Science

previously reported storage ceramics, the capacity of energy storage (75 kJ/L) has been decreased by more than two-thirds. However, the critical transition temperature from β to λ decreased substantially, thereby providing a wider range of applications, as shown in Fig. 6(d). It shows great potential for use in power plants through the

absorption of thermal energy from hot water. However, the relatively high pressure of the transformation from λ to β will be a challenge in practical applications.

SUN et al [67] reported Ti_3O_5 nano-film combined with carbon nano-tubes (CNTs)/Ni obtained by the PLD method under vacuum and

showed improved performance as super-capacitors due to the core-shell nano-structure of Ti_3O_5 @CNTs/Ni, as shown in Fig. 7. In contrast to those regular TiO_2 -based super-capacitors, Ti_3O_5 @CNTs/Ni showed an excellent specific capacitance of 445.7 F/g at a rate capacity of 1 A/g. The DFT calculation results indicated that the formation of Ti_3O_5 led to a substantial reduction in the band gap compared with TiO_2 .

The above observations strongly confirm

that Ti_3O_5 holds promise for energy storage applications.

4.3 Optical storage media

In 2010, OHKOSHI et al [27] synthesized nano-crystalline λ - Ti_3O_5 and showed photo-induced reversible properties between λ and β phases, as shown in Fig. 8. It was the firstly reported that Ti_3O_5 possessed photo-induced phase transition at room temperature. λ - Ti_3O_5 showed

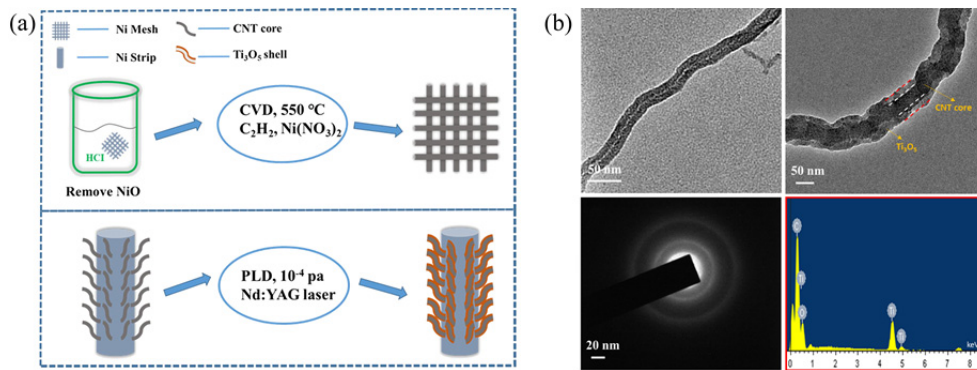


Fig. 7 (a) Schematic of material synthesis process; (b) Transmission electron microscopy images of core-shell nano-structure [67]. Reproduced with permission. Copyright 2021, Elsevier

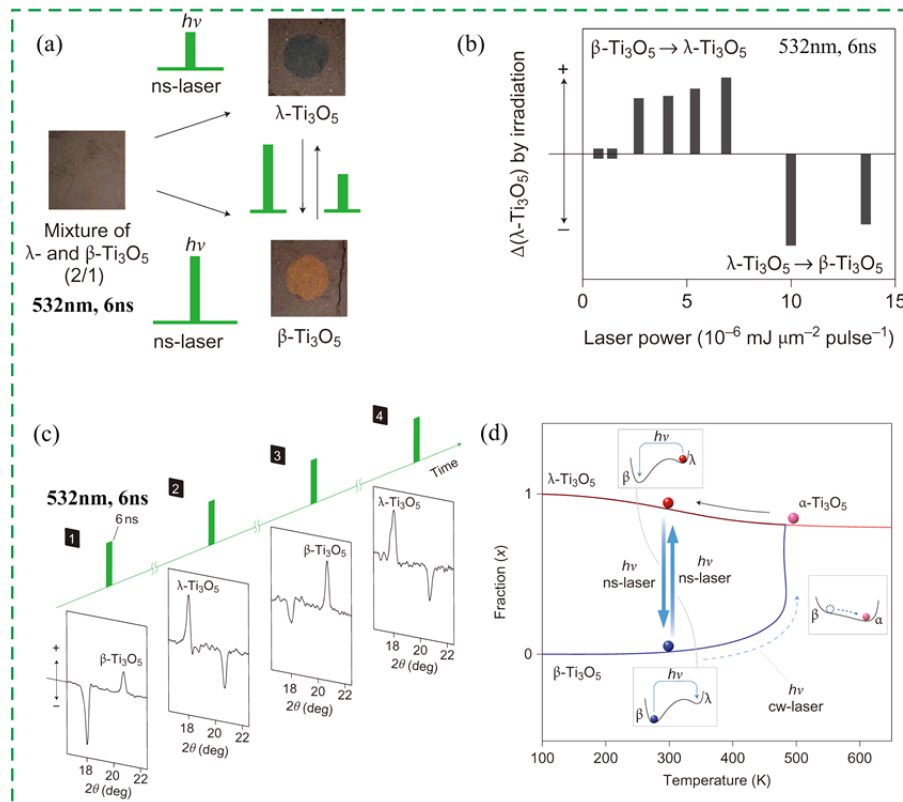


Fig. 8 (a) Reversible phase transition between λ and β induced by 532 nm pulsed laser light with different laser-power densities; (b) Variation in amount of λ - Ti_3O_5 ; (c) X-ray diffraction patterns of reversible phase transition; (d) Schematic of reversible phase transition induced by pulsed laser or continuous-wave (cw) laser [27]. Reproduced with permission. Copyright 2010, Nature

light absorption across a broad range of wavelengths, so the reversible phenomenon was observed under different incident nano-second-pulsed laser light (355, 532 and 1064 nm), which conferred Ti_3O_5 enormous potential in optical storage media. In addition, λ - Ti_3O_5 could also be obtained with continuous-wave laser irradiation from β - Ti_3O_5 to α - Ti_3O_5 to λ - Ti_3O_5 , as shown in Fig. 8(d). These features make Ti_3O_5 ideal for use as high-density optical memory devices, and the memory density is several hundred times greater than that of conventional devices.

To intrinsically understand the origin of the photo-induced performance of Ti_3O_5 , LIU et al [68] investigated the differences among the optical properties of materials using the DFT method. Results indicated that λ - Ti_3O_5 and β - Ti_3O_5 exhibited high variance across the visible spectrum in terms of absorption and reflectivity properties. The hard X-ray photo-electron spectroscopy results indicated that some satellites can be found in both the O and Ti spectra. These phenomena could arise not because of charge-transfer excitations but valence plasmon excitations [69]. To gain more insight into the mechanism, a time-resolved diffraction reflection technique was used to study the dynamic process of this phase transition. There is a threshold for the photo-induced phase transition from β to λ , and it begins within a few hundred femto-seconds with a non-thermal process [70]. The already formed λ -phase domains increased with a prolonged irradiation time, and a permanent phase transition was achieved when the particles were sufficiently large. Furthermore, the phase transition time induced by nano-second-pulsed or continuous-wave laser was estimated by a combination of single-shot time-resolved reflectivity measurements and Raman spectroscopy technologies. The reversible phase transition under nano-second pulse occurred at nano-second time scale ($\lambda \rightarrow \beta$: 900 ns; $\beta \rightarrow \lambda$: 20 ns); however, the λ to β transition under continuous-wave laser occurred at milli-second scale [71]. The aforementioned studies obtained several important findings, which provide novel insights into the photo-induced reversible properties of λ and β phases. However, all results were observed through indirect methods. After that, TASCA et al [72] directly observed the photo-induced process in structure with the excitation of a pulsed laser using a time-resolved powder XRD technique. A phase

transition from β to λ with a time faster than the experimental time resolution (10 μs) occurred, followed by a relaxation time of 20 μs . In 2021, MARIETTE et al [73] performed a more precise and complete characterization of this process using femto-second powder XRD, as shown in Fig. 9. They suggested that the photo-induced phase transition between λ and β phases was initiated by the propagation of elastic deformations rather than the initial nucleation and growth process. The stress caused by structural changes led to a strain wave that traveled at the speed of sound, eventually leading to the photo-induced phase transition.

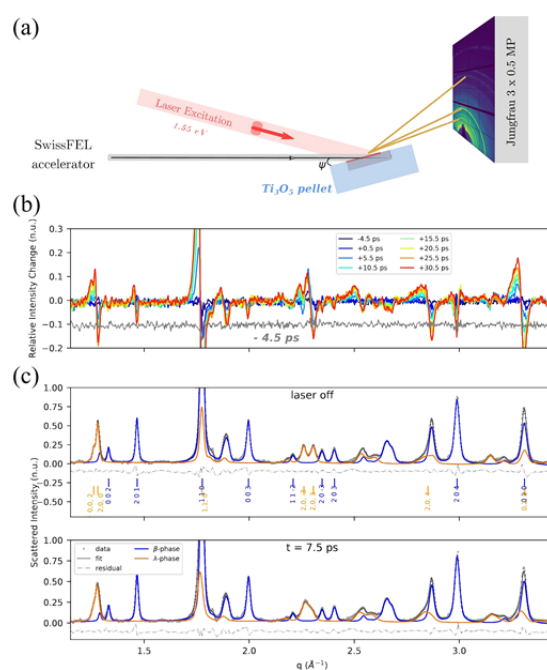


Fig. 9 (a) Experimental setup of time-resolved powder X-ray diffraction (XRD); (b) Relative intensive change of XRD patterns at different time scales; (c) Rietveld refinement results of XRD patterns for laser off and $t=7.5$ ps [73]. Reproduced with permission. Copyright 2021, Nature

4.4 Catalyst support

In recent years, the application of titanium sub-oxides, such as Ti_4O_7 , Ti_6O_{11} and Ti_8O_{15} , in chemical catalysts has been extensively studied due to their excellent performance in electrical conductivity, corrosion resistance and high-temperature stability [74–79]. Similarly, Ti_3O_5 also exhibits tremendous potential for use in electrode and catalyst support materials owing to its better electro-chemical activities and stability towards strong acids and bases [80].

Some researchers have discovered the potential application of Ti_3O_5 when they introduce Ti_3O_5 as catalyst support for fuel cells for cathodic oxygen reduction [81–84]. ALIPOUR MOGHADAM ESFAHANI et al [85] synthesized Ti_3O_5 -Mo carbon-free support for platinum-based catalyst proton exchange membrane fuel cells (PEMFCs), as shown in Fig. 10. Significant high catalyst activity of 73 mA/mg (Pt) at a current density of 1.1 mA/cm² and 0.9 V was observed for Mo-doped Ti_3O_5 , followed by that of commercial Pt/C catalyst support [86,87]. The enhanced catalyst activity was due to the combined effect of oxygen vacancies and Ti^{3+} defects in Ti_3O_5 . Stability and durability were also significantly improved compared to commercial Pt/C from the results of potential cycling and ultraviolet-visible (UV-Vis) measurements of electrolytes. After that, they introduced Mo and Si into Ti_3O_5 ($\text{Ti}_3\text{O}_5\text{Mo}_{0.2}\text{Si}_{0.4}$), showing improved performance compared with previous results (1.57 mA/cm² at 0.9 V) [29,88]. Recently, ALIPOUR MOGHADAM ESFAHANI et al [89] have introduced N-functional groups into Ti_3O_5 -Mo to improve catalyst activity and stability. To ensure catalyst activity, they further investigated the durability of Pt/ $\text{Ti}_3\text{O}_5\text{Mo}_{0.2}\text{Si}_{0.4}$ using multiple accelerated stress tests and found that the support not only stabilizes the catalyst but also ensures the effectiveness of active sites [90].

In addition to its application in PEMFCs, Pt/ $\text{Ti}_3\text{O}_5\text{Mo}_{0.2}\text{Si}_{0.4}$ could be extended to direct methanol fuel cells (DMFCs). Excellent activities were found in methanol oxidation reactions, which were the major reaction in anodes of DMFCs [91]. A significantly higher current density of 58.92 mA/cm² was observed for Pt/ $\text{Ti}_3\text{O}_5\text{Mo}_{0.2}\text{Si}_{0.4}$, followed by those of Pt/C catalysts. In addition, the activation energy for related reactions considerably decreased, simultaneously showing higher exchange current densities.

SHI et al [92] prepared $\text{Ti}_4\text{O}_7/\lambda\text{-Ti}_3\text{O}_5$ dual-phase nano-fibers using the hydro-thermal reaction method and used them in the oxygen reduction reaction. Ti_4O_7 and $\lambda\text{-Ti}_3\text{O}_5$ in this structure exhibit mutual synergies in catalytic activity compared with the single-phase, providing a new idea for developing electrocatalysts. This material showed good performance in terms of methanol tolerance and cyclic stability. However, electrocatalytic performance should be further improved.

4.5 Photocatalysis

Titanium suboxides, such as Ti_2O_3 , Ti_3O_5 , Ti_4O_7 and Ti_8O_{15} , exhibit certain photo-activities due to existence of oxygen vacancies [13,93–96]. STEM et al [97] synthesized micro-scale Ti_3O_5 on silicon substrates using carbon-doped TiO_2 thin films as a precursor, and the schematic illustration of prepared micro-scale meshes is shown in Fig. 11. Under visible light, it showed better absorbance and photo-luminescence emission performance due to defects within Ti_3O_5 introduced by doped carbon. Using the same method, they also prepared Ti_3O_5 thin film containing 75 wt% $\lambda\text{-Ti}_3\text{O}_5$, 25 wt% TiO_2 (rutile) and trace $\text{TiO}_{2-x}\text{C}_x$ and it is expected to be useful in solar cells and photo-catalysis [98].

QI et al [99] reported Ti_3O_5 as a catalyst for photo-degradation. Ti_3O_5 nano-rods were obtained by treating Ti_5Si_3 powders in O_2 flow at 800 °C for 90 min. Under the UV-Vis condition, the Ti_3O_5 nano-rods showed a good degradation effect towards methylene blue solutions, and the degradation rate could reach up to 80.0% [99].

4.6 Superconductivity

Excellent superconductivity performance was found by YOSHIMATSU et al [100] in $\gamma\text{-Ti}_3\text{O}_5$ thin films, with the highest super-conducting transition temperature of 7.1 K among simple oxides. These thin films were prepared using PLD method on

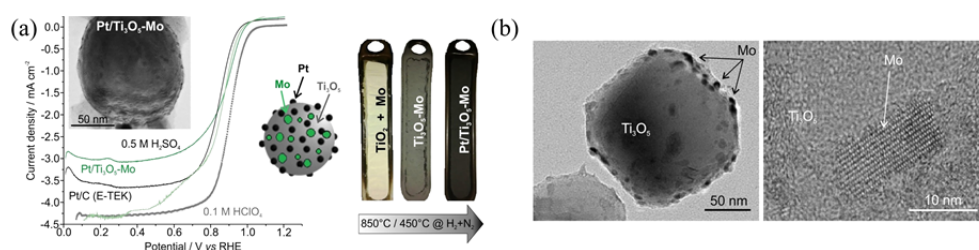


Fig. 10 (a) Schematic of material synthesis process; (b) Transmission electron microscopy images of Ti_3O_5 -Mo support [85]. Reproduced with permission. Copyright 2017, Elsevier

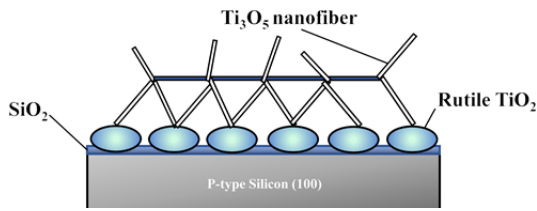


Fig. 11 Schematic of Ti_3O_5 nano-fiber on silicon substrate [97]. Reproduced with permission. Copyright 2011, Elsevier

different substrates, and their properties were considerably influenced by the atmosphere around the substrates. The superconductivity properties were attributed to bipolaronic superconductivity, which has much to do with oxygen non-stoichiometry and epitaxial stabilization. After that, they investigated in more depth the mechanism of superconductivity performance of $\gamma\text{-Ti}_3\text{O}_5$ by regulating the structure phase transformation [19]. A super-conducting phase diagram containing TiO , Ti_2O_3 and $\gamma\text{-Ti}_3\text{O}_5$ was created on the basis of the experimental results to clarify the superconducting state arising from $\gamma\text{-Ti}_3\text{O}_5$.

FAN et al [20] grew a series of Ti_3O_5 thin films on $\alpha\text{-Al}_2\text{O}_3$ substrates using the PLD method by controlling oxygen pressure (from 4×10^{-4} to 1×10^{-3} Pa). $\gamma\text{-Ti}_3\text{O}_5$ was prepared when the oxygen

concentration reached 1×10^{-3} Pa. However, no superconductivity phenomenon was found, as shown in Fig. 12 [20]. Thus, further experiments need to be conducted to investigate the detailed mechanisms.

4.7 Other application

Excellent microwave absorption performance was observed in $\lambda\text{-Ti}_3\text{O}_5$ and Li-doped $\lambda\text{-Ti}_3\text{O}_5$ due to the multivalent characteristic of Ti ions [101]. Three Ti ions with different valence states formed different micro-electric fields in the materials, which will improve the microwave absorption performance in a broad frequency range. Thus, the as-prepared $\lambda\text{-Ti}_3\text{O}_5$ showed a higher efficient absorption bandwidth than most of the other oxide-based microwave absorbing materials. In addition, Li-doped $\lambda\text{-Ti}_3\text{O}_5$ showed the highest E_{AB}/d values (E_{AB} is the effective absorption bandwith; d is the sample thickness) due to the formation of the Li–O micro-electric field.

LI et al [102] synthesized $\gamma\text{-Ti}_3\text{O}_5$ by hydrogen reduction of hierarchical micro-spheres of TiO_2 , as shown in Fig. 13, and used it as the substrate of surface-enhanced Raman scattering (SERS). The as-prepared substrate exhibited a lower limit of detection (10^{-10} mol/L) for Rhodamine 6G and

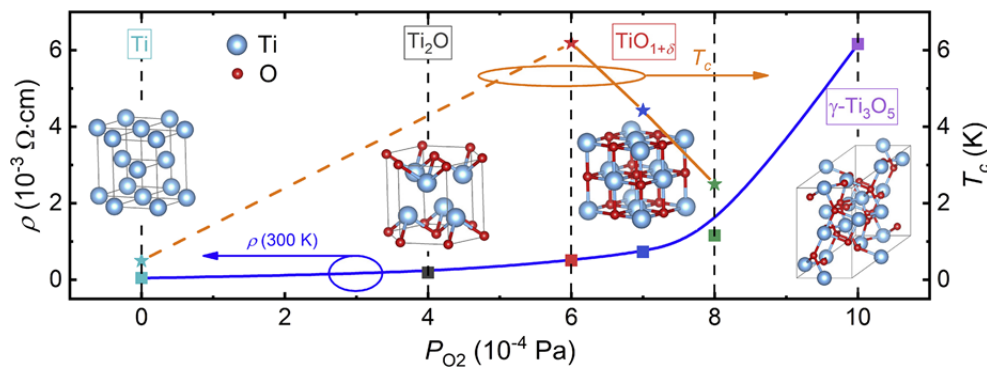


Fig. 12 Super-conducting properties of Ti bulk and trititanium pentoxide (Ti_3O_5) films at different oxygen pressures. Squares: 300 K; Stars: T_c [20]. Reproduced with permission. Copyright 2019, Elsevier

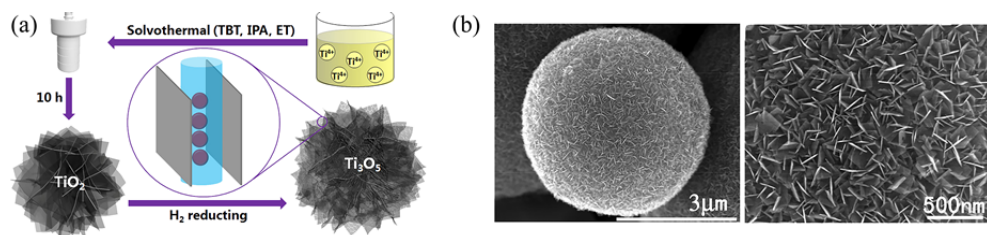


Fig. 13 (a) Schematic of material synthesis process; (b) Scanning electron microscopy images of hierarchical micro-spheres of $\gamma\text{-Ti}_3\text{O}_5$ [102]. Reproduced with permission. Copyright 2019, American Chemical Society

excellent stability performance under conditions of high-temperature oxidation and concentrated alkali and acid with a high specific area of 405.8 m²/g. In addition, it still showed good SERS activity after several cycles of use. Compared with TiO₂ substrates, γ -Ti₃O₅ had improved detection sensitivity as high as 10000-fold.

DING et al [103] synthesized Ti₃O₅/Ti₄O₇ nano-fibers by hydro-thermal method and used them as adsorbents to capture SARS-CoV-2b (severe acute respiratory syndrome coronavirus 2) for further detection or to scavenge it from the environment. These dual-phase adsorbents exhibited a high affinity for proteins or phospholipids. Compared with Ti₆O₁₁, they showed improved adsorption and efficient performance with lower virus concentrations after adsorption. This study provided a new way for practical applications of Ti₃O₅.

5 Summary and perspective

Over a couple of decades, a considerable research effort has gone into the crystal structure, preparation methods, physical and chemical properties and applications of Ti₃O₅. There has been an exhaustive understanding of different Ti₃O₅ crystalline forms (α , β , γ , δ and λ) in terms of physical and chemical properties, and the change in physical properties that have resulted from phase transitions between these forms. Such properties confer Ti₃O₅ potential interest for use in gas sensors, photo-catalysis, catalyst support, superconductivity, etc. Especially, the unique pressure–heat, pressure–light and pressure–current reversible phase transitions between λ - and β -Ti₃O₅ with different external stimulations have been piquing increasing research interest. These also offer new applications of Ti₃O₅ in the field of energy and data storage. In addition, several new methods have also been proposed for preparing Ti₃O₅ with high quality and different grain sizes. In practice, different grain sizes have a significant impact on the room temperature stability, phase transition and heat storage performance of λ -Ti₃O₅. However, further work to understand the phase-transition mechanism between λ and β phases is required. More recently, Ti₃O₅ has shown amazing application potential in the fields of trace detection, microwave absorption and virus adsorption, which further broadens the

application range of Ti₃O₅. Therefore, Ti₃O₅ is expected to be a multi-purpose material in the future.

Nowadays, there are sufficient research and understanding of the basic physicochemical properties for different crystal forms of Ti₃O₅. Thus, the future research focus would be how to develop new applications of Ti₃O₅ in the field of energy utilization and conversion.

Acknowledgments

The authors would like to thank the financial supports from the National Natural Science Foundation of China (Nos. 52004157, U1860203, 52022054, 51974181), the Shanghai Sailing Program, China (No. 21YF1412900), the Shanghai Rising-Star Program, China (No. 19QA1403600), the Shanghai Engineering Research Center of Green Remanufacture of Metal Parts, China (No. 19DZ2252900), the Program for Professor of Special Appointment (Eastern Scholar) at Shanghai Institutions of Higher Learning, China (No. TP2019041), the “Shuguang Program” supported by the Shanghai Education Development Foundation and the Shanghai Municipal Education Commission, China (No. 21SG42), the Independent Research and Development Project of State Key Laboratory of Advanced Special Steel, Shanghai Key Laboratory of Advanced Ferrometallurgy, Shanghai University, China (No. SKLASS 2020-Z10), and the Science and Technology Commission of Shanghai Municipality, China (No. 19DZ2270200).

References

- [1] SHAYAN M, EGHBALI B, NIROUMAND B. Fabrication of AA2024–TiO₂ nanocomposites through stir casting process [J]. Transactions of Nonferrous Metals Society of China, 2020, 30: 2891–2903.
- [2] YUMAK N, ASLANTAŞ K. A review on heat treatment efficiency in metastable β titanium alloys: The role of treatment process and parameters [J]. Journal of Materials Research and Technology, 2020, 9: 15360–15380.
- [3] ZHENG Li, SHI Qian, LIU Xuan-yong. Induced antibacterial capability of TiO₂ coatings in visible light via nitrogen ion implantation [J]. Transactions of Nonferrous Metals Society of China, 2020, 30: 171–180.
- [4] DU Yu-xuan, YANG Xin-liang, LI Zu-shu, HAO Fang, MAO You-chuan, LI Shao-qiang, LIU Xiang-hong, FENG Yong, YAN Zhi-ming. Shear localization behavior in hat-shaped specimen of near- α Ti–6Al–2Zr–1Mo–1V titanium alloy loaded at high strain rate [J]. Transactions of

- Nonferrous Metals Society of China, 2021, 31: 1641–1655.
- [5] SHI Xiao-hui, CAO Zu-han, FAN Zhi-yuan, ECKERT J, QIAO Jun-wei. Static coarsening behavior of equiaxed α phase in Ti–8Al–1Mo–1V alloy [J]. Transactions of Nonferrous Metals Society of China, 2021, 31: 1628–1640.
- [6] ZOU Cheng-xiong, LI Jin-shan, WANG William-yi, ZHANG Ying, LIN De-ye, YUAN Rui-hao, WANG Xiao-dan, TANG Bin, WANG Jun, GAO Xing-yu. Integrating data mining and machine learning to discover high-strength ductile titanium alloys [J]. Acta Materialia, 2021, 202: 211–221.
- [7] GAO Yang, YIN Zhi-bin, JI Qian, JIANG Jia-bing, TAO Zheng-zheng, ZHAO Xiao-long, SUN Si-jia, WU Ai-guo, ZENG Le-yong. Black titanium dioxide@manganese dioxide for glutathione-responsive MR imaging and enhanced photothermal therapy [J]. Journal of Materials Chemistry B, 2021, 9: 314–321.
- [8] SU Yue, ZHANG Wei, CHEN Shan-ming, YAO Dan-wen, XU Ji-lian, CHEN Xiao-bo, LIU Lei, XU Huai-liang. Engineering black titanium dioxide by femtosecond laser filament [J]. Applied Surface Science, 2020, 520: 146298.
- [9] LIU Xing-xin, YU Xiao-yan, SHA Li, WANG Yu-qian, ZHOU Zhuo, ZHANG Shu-ting. The preparation of black titanium oxide nanoarray via coking fluorinated wastewater and application on coking wastewater treatment [J]. Chemosphere, 2021, 270: 128609.
- [10] YU Min, SAUNDERS T, GRASSO S, MAHAJAN A, ZHANG Hang-feng, REECE M J. Magnéli phase titanium suboxides by flash spark plasma sintering [J]. Scripta Materialia, 2018, 146: 241–245.
- [11] CANCAREVIC M, ZINKEVICH M, ALDINGER F. Thermodynamic description of the Ti–O system using the associate model for the liquid phase [J]. Calphad, 2007, 31: 330–342.
- [12] OKAMOTO H. O–Ti (oxygen–titanium) [J]. Journal of Phase Equilibria and Diffusion, 2011, 32: 473–474.
- [13] DOMASCHKE M, ZHOU Xue-mei, WERGEN L, ROMEIS S, MIEHLICH M E, MEYER K, PEUKERT W, SCHMUKI P. Magnéli-phases in anatase strongly promote cocatalyst-free photocatalytic hydrogen evolution [J]. ACS Catalysis, 2019, 9: 3627–3632.
- [14] MALIK H, SARKAR S, MOHANTY S, CARLSON K. Modelling and synthesis of Magnéli phases in ordered titanium oxide nanotubes with preserved morphology [J]. Scientific Reports, 2020, 10: 8050.
- [15] van LANDUYT J, AMELINCKX S. On the generation mechanism for shear planes in shear structures [J]. Journal of Solid State Chemistry, 1973, 6: 222–229.
- [16] ANDERSSON S, COLLÉN B, KUYLENSTIERNA U, MAGNÉLI A. Phase analysis studies on the titanium–oxygen system [J]. Acta Chemica Scandinavica, 1957, 11: 1641–1652.
- [17] SHI Qi-wu, CHAI Guo-qing, HUANG Wan-xia, SHI Yan-li, HUANG Bo, WEI Dan, QI Jian-qi, SU Fu-hai, XU Wen, LU Tie-cheng. Fabrication of nanocrystalline λ -Ti₃O₅ with tunable terahertz wave transmission properties across a temperature induced phase transition [J]. Journal of Materials Chemistry C, 2016, 4: 10279–10285.
- [18] ÅSBRINK S, MAGNÉLI A. Note on the crystal structure of trititanium pentoxide [J]. Acta Chemica Scandinavica, 1957, 11: 1606–1607.
- [19] KUROKAWA H, YOSHIMATSU K, SAKATA O, OHTOMO A. Effects of phase fraction on superconductivity of low-valence eutectic titanate films [J]. Journal of Applied Physics, 2017, 122: 055302.
- [20] FAN Yun-jie, ZHANG Chao, LIU Xiang, LIN Yue, GAO Guan-yin, MA Chao, YIN Yue-wei, LI Xiao-guang. Structure and transport properties of titanium oxide (Ti₂O, TiO_{1+ δ} , and Ti₃O₅) thin films [J]. Journal of Alloys and Compounds, 2019, 786: 607–613.
- [21] KITADA A, HASEGAWA G, KOBAYASHI Y, KANAMORI K, NAKANISHI K, KAGEYAMA H. Selective preparation of macroporous monoliths of conductive titanium oxides Ti_nO_{2n–1} (n=2, 3, 4, 6) [J]. Journal of the American Chemical Society, 2012, 134: 10894–10898.
- [22] CHAI Guo-qing, HUANG Wan-xia, SHI Qi-wu, ZHENG Shu-ping, WEI Dan. Preparation and characterization of λ -Ti₃O₅ by carbothermal reduction of TiO₂ [J]. Journal of Alloys and Compounds, 2015, 621: 404–410.
- [23] CAI Yu, SHI Qi-wu, WANG Ming-zhe, LV Xiang, CHENG Ye, HUANG Wan-xia. Synthesis of nanoscale λ -Ti₃O₅ via a PEG assisted sol–gel method [J]. Journal of Alloys and Compounds, 2020, 848: 156585.
- [24] YANG Shun-shun, ZHANG Le, MA Yue-long, SUN Bing-heng, SHAN Yin-shuang, SHI Ze-di, ZHOU Tian-yuan, WANG Yun, SELIM F A, LI Yan-bin. A novel carbon thermal reduction approach to prepare recorded purity β -Ti₃O₅ compacts from titanium dioxide and phenolic resin [J]. Journal of Alloys and Compounds, 2021, 853: 157360.
- [25] IWASAKI H, BRIGHT N F H, ROWLAND J F. The polymorphism of the oxide Ti₃O₅ [J]. Journal of the Less Common Metals, 1969, 17: 99–110.
- [26] ZHENG Liao-ying. The oxygen sensing properties and mechanisms of M-doped α -Ti₃O₅ thin films (M= Ce, W ions) [J]. Sensors and Actuators B: Chemical, 2003, 94: 294–297.
- [27] OHKOSHI S I, TSUNOBUCHI Y, MATSUDA T, HASHIMOTO K, NAMAI A, HAKOE F, TOKORO H. Synthesis of a metal oxide with a room-temperature photoreversible phase transition [J]. Nature chemistry, 2010, 2: 539–545.
- [28] NASU T, TOKORO H, TANAKA K, HAKOE F, NAMAI A, OHKOSHI S. Sol–gel synthesis of nanosized λ -Ti₃O₅ crystals [J]. IOP Conference Series: Materials Science and Engineering, 2014, 54: 012008.
- [29] ALIPOUR MOGHADAM ESFAHANI R, RIVERA GAVIDIA L M, GARCÍA G, PASTOR E, SPECCHIA S. Highly active platinum supported on Mo-doped titanium nanotubes suboxide (Pt/TNTS–Mo) electrocatalyst for oxygen reduction reaction in PEMFC [J]. Renewable Energy, 2018, 120: 209–219.
- [30] BARTHOLOMEW R F, WHITE W B. Growth of the intermediate oxides of titanium from borate fluxes under controlled oxygen fugacities [J]. Journal of Crystal Growth, 1970, 6: 249–252.
- [31] CHEN G Z, FRAY D J, FARTHING T W. Direct electrochemical reduction of titanium dioxide to titanium in molten calcium chloride [J]. Nature, 2000, 407: 361–364.
- [32] WANG Bin, LIU Kui-ren, CHEN Jian-she. Reaction mechanism of preparation of titanium by electro-deoxidation in molten salt [J]. Transactions of Nonferrous Metals Society of China, 2011, 21: 2327–2331.

- [33] DRING K, DASHWOOD R, INMAN D. Voltammetry of titanium dioxide in molten calcium chloride at 900 °C [J]. *Journal of the Electrochemical Society*, 2005, 152: E104.
- [34] DRING K, DASHWOOD R, INMAN D. Predominance diagrams for electrochemical reduction of titanium oxides in molten CaCl₂ [J]. *Journal of the Electrochemical Society*, 2005, 152: D184.
- [35] KAR P, EVANS J W. Determination of kinetic parameters by modeling of voltammograms for electrochemical reduction of titanium dioxide [J]. *Electrochemistry communications*, 2006, 8: 1397–1403.
- [36] ERTEKIN Z, TAMER U, PEKMEZ K. Cathodic electrochemical deposition of Magnéli phases Ti_nO_{2n-1} thin films at different temperatures in acetonitrile solution [J]. *Electrochimica Acta*, 2015, 163: 77–81.
- [37] ERTEKIN Z, PEKMEZ N Ö, PEKMEZ K. One-step electrochemical deposition of thin film titanium suboxide in basic titanyl sulfate solution at room temperature [J]. *Journal of Solid State Electrochemistry*, 2020, 24: 975–986.
- [38] PESHEV P, IVANOVA M. Growth of Ti₂O₃ single crystals by a chemical transport reaction [J]. *Physica Status Solidi (a)*, 1975, 28: K1–K4.
- [39] MERCIER J, SINCE J J, FOURCAUDOT G, DUMAS J, DEVENYI J. Growth and characterization of titanium suboxide crystals [J]. *Journal of Crystal Growth*, 1977, 42: 583–587.
- [40] STROBEL P, PAGE Y. Crystal growth of Ti_nO_{2n-1} oxides (*n*=2 to 9) [J]. *Journal of Materials Science*, 1982, 17: 2424–2430.
- [41] HONG S H. Crystal growth of some intermediate titanium oxide phases γ -Ti₃O₅, β -Ti₃O₅, Ti₄O₇, and Ti₂O₃ by chemical transport reactions [J]. *Acta Chem Scand*, 1982, 207–217.
- [42] HONG S H, ÅSBRINK S. The structure of γ -Ti₃O₅ at 297 K [J]. *Acta Crystallographica (Section B): Structural Crystallography and Crystal Chemistry*, 1982, 38: 2570–2576.
- [43] ÅSBRINK S, MAGNÉLI A. Crystal structure studies on trititanium pentoxide, Ti₃O₅ [J]. *Acta Crystallographica*, 1959, 12: 575–581.
- [44] ONODA M, OGAWA Y, TAKI K. Phase transitions and the doping effect in Ti₃O₅ [J]. *Journal of Physics: Condensed Matter*, 1998, 10: 7003.
- [45] ÅSBRINK G, ÅSBRINK S, MAGNELI A, OKINAKA H, KOSUGE K, KACHI S. Ti₃O₅ modification of V₃O₅-type structure [J]. *Acta Chemica Scandinavica*, 1971, 25: 3889–3890.
- [46] TANAKA K, NASU T, MIYAMOTO Y, OZAKI N, TANAKA S, NAGATA T, HAKOE F, YOSHIKIYO M, NAKAGAWA K, UMETA Y, IMOTO K, TOKORO H, NAMAI A, OHKOSHI S I. Structural phase transition between γ -Ti₃O₅ and δ -Ti₃O₅ by breaking of a one-dimensionally conducting pathway [J]. *Crystal Growth & Design*, 2015, 15: 653–657.
- [47] RAO C N R, RAMDAS S, LOEHMAN R E, HONIG J M. Semiconductor-metal transition in Ti₃O₅ [J]. *Journal of Solid State Chemistry*, 1971, 3: 83–88.
- [48] KEYS L K. Magnetic studies of Ti₃O₅ [J]. *Physics Letters A*, 1967, 24: 628–630.
- [49] ONODA M. Phase transitions of Ti₃O₅ [J]. *Journal of Solid State Chemistry*, 1998, 136: 67–73.
- [50] GREY I E, WARD J. An X-ray and Mossbauer study of the FeTi₂O₅–Ti₃O₅ system [J]. *Journal of Solid State Chemistry*, 1973, 7: 300–307.
- [51] KELLERMAN D G. Effect of doping on the phase transition in Ti₃O₅ [J]. *Journal of Inorganic Materials*, 1983, 19: 221.
- [52] WECHSLER B A, NAVROTSKY A. Thermodynamics and structural chemistry of compounds in the system MgO–TiO₂ [J]. *Journal of Solid State Chemistry*, 1984, 55: 165–180.
- [53] STEINER H J, TURRILLAS X, STEELE B C H. Phase relationships and electrical properties of Ti₃O₅, CrTi₂O₅ and the pseudobrookite-type systems Mg_xTi_{3-x}O₅ and Li_xTi_{3-x}O₅ [J]. *Journal of Materials Chemistry*, 1992, 2: 1249–1256.
- [54] GREY I E, LI C, MADSEN I C. Phase equilibria and structural studies on the solid solution MgTi₂O₅–Ti₃O₅ [J]. *Journal of Solid State Chemistry*, 1994, 113: 62–73.
- [55] TAKAHAMA R, ISHII T, INDO D, ARIZONO M, TERAKURA C, TOKURA Y, TAKESHITA N, NODA M, KUWAHARA H, SAIKI T, KATSUFUJI T, KAJIMOTO R, OKUDA T. Structural, magnetic, transport, and thermoelectric properties of the pseudobrookite AlTi₂O₅–Ti₃O₅ system [J]. *Physical Review Materials*, 2020, 4: 074401.
- [56] MAKIURA R, TAKABAYASHI Y, FITCH A N, TOKORO H, OHKOSHI S I, PRASSIDES K. Nanoscale effects on the stability of the λ -Ti₃O₅ polymorph [J]. *Chemistry—An Asian Journal*, 2011, 6: 1886–1890.
- [57] HUANG Bo, HUANG Wan-xia, SHI Qi-wu, ZHENG Shu-ping, SHEN Zu-jia. The preparation and phase transformation characteristics of γ -Ti₃O₅ thin film [J]. *Journal of Materials Science: Materials in Electronics*, 2017, 28: 7868–7873.
- [58] ZHENG Liao-ying. The preparation and oxygen-sensing properties of α -Ti₃O₅ thin film [J]. *Sensors and Actuators B: Chemical*, 2003, 88: 115–119.
- [59] ZHANG Xiao-yan, LIU Wan-ying, YU Hua, ZHONG Xiao-xi, WANG Li-jun, SINGH A, LIN Yuan-hua. Preparation and oxygen sensing properties of Ti₃O₅ submicron rods [J]. *Micro & Nano Letters*, 2016, 11: 811–813.
- [60] LI Xiao-lei, LIU Ying, MA Shi-qing, YE Jin-wen, ZHANG Xiao-yan, WANG Guang-wei, QIU Yu-chong. The synthesis and gas sensitivity of the β -Ti₃O₅ powder: Experimental and DFT study [J]. *Journal of Alloys and Compounds*, 2015, 649: 939–948.
- [61] TOKORO H, YOSHIKIYO M, IMOTO K, NAMAI A, NASU T, NAKAGAWA K, OZAKI N, HAKOE F, TANAKA K, CHIBA K J, MAKIURA R, PRASSIDES K, OHKOSHI S I. External stimulation-controllable heat-storage ceramics [J]. *Nature Communications*, 2015, 6: 7037.
- [62] WEI Dan, HUANG Wan-xia, SHI Qi-wu, LU Tie-cheng, HUANG Bo. Effect of coating layers on nano-TiO₂ particles on the preparation of nanocrystalline λ -Ti₃O₅ by carbonthermal reduction [J]. *Journal of Materials Science: Materials in Electronics*, 2016, 27: 4216–4222.
- [63] SHEN Zu-jia, SHI Qi-wu, HUANG Wan-xia, HUANG Bo, WANG Ming-zhe, GAO Jun-zheng, SHI Yan-li, LU Tie-cheng. Stabilization of microcrystal λ -Ti₃O₅ at room temperature by aluminum-ion doping [J]. *Applied Physics Letters*, 2017, 111: 191902.
- [64] WANG Ming-zhe, HUANG Wan-xia, SHEN Zu-jia, GAO

- Jun-zheng, SHI Yan-li, LU Tie-cheng, SHI Qi-wu. Phase evolution and formation of λ phase in Ti_3O_5 induced by magnesium doping [J]. *Journal of Alloys and Compounds*, 2019, 774: 1189–1194.
- [65] OHKOSHI S I, TOKORO H, NAKAGAWA K, YOSHIKIYO M, JIA F, NAMAI A. Low-pressure-responsive heat-storage ceramics for automobiles [J]. *Scientific Reports*, 2019, 9: 13203.
- [66] NAKAMURA Y, SAKAI Y, AZUMA M, OHKOSHI S I. Long-term heat-storage ceramics absorbing thermal energy from hot water [J]. *Science Advances*, 2020, 6: eaaz5264.
- [67] SUN Peng, HU Xue-yan, WEI Guang-feng, WANG Rui-jing, WANG Qiang, WANG Huan-wen, WANG Xue-feng. Ti_3O_5 nanofilm on carbon nanotubes by pulse laser deposition: Enhanced electrochemical performance [J]. *Applied Surface Science*, 2021, 548: 149269.
- [68] LIU Rui, SHANG Jia-xiang, WANG Fu-he. Electronic, magnetic and optical properties of β - Ti_3O_5 and λ - Ti_3O_5 : A density functional study [J]. *Computational Materials Science*, 2014, 81: 158–162.
- [69] KOBAYASHI K, TAGUCHI M, KOBATA M, TANAKA K, TOKORO H, DAIMON H, OKANE T, YAMAGAMI H, IKENAGA E, OHKOSHI S I. Electronic structure and correlation in β - Ti_3O_5 and λ - Ti_3O_5 studied by hard X-ray photoelectron spectroscopy [J]. *Physical Review B*, 2017, 95: 085133.
- [70] ASAHARA A, WATANABE H, TOKORO H, OHKOSHI S I, SUEMOTO T. Ultrafast dynamics of photoinduced semiconductor-to-metal transition in the optical switching nano-oxide Ti_3O_5 [J]. *Physical Review B*, 2014, 90: 014303.
- [71] OULD-HAMOUDA A, TOKORO H, OHKOSHI S I, FREYSZ E. Single-shot time resolved study of the photo-reversible phase transition induced in flakes of Ti_3O_5 nanoparticles at room temperature [J]. *Chemical Physics Letters*, 2014, 608: 106–112.
- [72] TASCA K R, ESPOSITO V, LANTZ G, BEAUD P, KUBLI M, SAVOINI M, GILES C, JOHNSON S L. Time-resolved X-ray powder diffraction study of photoinduced phase transitions in Ti_3O_5 nanoparticles [J]. *ChemPhysChem*, 2017, 18: 1385–1392.
- [73] MARIETTE C, LORENC M, CAILLEAU H, et al. Strain wave pathway to semiconductor-to-metal transition revealed by time-resolved X-ray powder diffraction [J]. *Nature Communications*, 2021, 12: 1239.
- [74] WALSH F C, WILLS R G A. The continuing development of Magnéli phase titanium sub-oxides and Ebonex[®] electrodes [J]. *Electrochimica Acta*, 2010, 55: 6342–6351.
- [75] LIN Hui, XIAO Run-lin, XIE Ru-zhen, YANG Li-hui, TANG Cai-ming, WANG Rong-rong, CHEN Jie, LV Si-hao, HUANG Qing-guo. Defect engineering on a Ti_4O_7 electrode by Ce^{3+} doping for the efficient electrooxidation of perfluorooctanesulfonate [J]. *Environmental Science & Technology*, 2021, 55: 2597–2607.
- [76] LIU Meng-ting, JHULKI S, SUN Zi-fei, MAGASINSKI A, HENDRIX C, YUSHIN G. Atom-economic synthesis of Magnéli phase Ti_4O_7 microspheres for improved sulfur cathodes for Li-S batteries [J]. *Nano Energy*, 2021, 79: 105428.
- [77] HE Chun-yong, CHANG Shi-yong, HUANG Xiang-dong, WANG Qing-quan, MEI Ao, SHEN Pei-kang. Direct synthesis of pure single-crystalline Magnéli phase Ti_8O_{15} nanowires as conductive carbon-free materials for electrocatalysis [J]. *Nanoscale*, 2015, 7: 2856–2861.
- [78] SHEN Pei-kang, HE Chun-yong, CHANG Shi-yong, HUANG Xiang-dong, TIAN Zhi-qun. Magnéli phase Ti_8O_{15} nanowires as conductive carbon-free energy materials to enhance the electrochemical activity of palladium nanoparticles for direct ethanol oxidation [J]. *Journal of Materials Chemistry A*, 2015, 3: 14416–14423.
- [79] LEE G W, PARK B H, NAZARIAN-SAMANI M, KIM Y H, ROH K C, KIM K B. Magnéli phase titanium oxide as a novel anode material for potassium-ion batteries [J]. *ACS Omega*, 2019, 4: 5304–5309.
- [80] WANG Li-jun, ZHANG Xiao-yan, LIU Wan-ying, XU Wen, SINGH A, LIN Yuan-hua. Electrochemical properties of Ti_3O_5 powders prepared by carbothermal reduction [J]. *Journal of Materials Science: Materials in Electronics*, 2017, 28: 6421–6425.
- [81] IGNASZAK A, SONG Chao-jie, ZHU Wei-min, ZHANG Jiu-jun, BAUER A, BAKER R, NEBURCHILOV V, YE Si-yu, CAMPBELL S. Titanium carbide and its core-shelled derivative TiC@TiO_2 as catalyst supports for proton exchange membrane fuel cells [J]. *Electrochimica Acta*, 2012, 69: 397–405.
- [82] NGUYEN T T, HO V T T, PAN C J, LIU J Y, CHOU H L, RICK J, SU W N, HWANG B J. Synthesis of $\text{Ti}_{0.7}\text{Mo}_{0.3}\text{O}_2$ supported-Pt nanodendrites and their catalytic activity and stability for oxygen reduction reaction [J]. *Applied Catalysis B: Environmental*, 2014, 154/155: 183–189.
- [83] LORI O, ELBAZ L. Advances in ceramic supports for polymer electrolyte fuel cells [J]. *Catalysts*, 2015, 5: 1445–1464.
- [84] ALIPOUR MOGHADAM ESFAHANI R, MONTEVERDE VIDELA A H A, VANKOVA S, SPECCHIA S. Stable and methanol tolerant Pt/TiO_x -C electrocatalysts for the oxygen reduction reaction [J]. *International Journal of Hydrogen Energy*, 2015, 40: 14529–14539.
- [85] ALIPOUR MOGHADAM ESFAHANI R, VANKOVA S K, MONTEVERDE VIDELA A H A, SPECCHIA S. Innovative carbon-free low content Pt catalyst supported on Mo-doped titanium suboxide (Ti_3O_5 -Mo) for stable and durable oxygen reduction reaction [J]. *Applied Catalysis B: Environmental*, 2017, 201: 419–429.
- [86] PARRONDO J, HAN T, NIANGAR E, WANG C, DALE N, ADJEMIAN K, RAMANI V. Platinum supported on titanium-ruthenium oxide is a remarkably stable electrocatalyst for hydrogen fuel cell vehicles [J]. *Proceedings of the National Academy of Sciences of the United States of America*, 2014, 111: 45–50.
- [87] WANG Gong-wei, HUANG Bing, XIAO Li, REN Zhan-dong, CHEN Hao, WANG De-li, ABRUÑA H D, LU Jun-tao, ZHUANG Lin. Pt Skin on AuCu intermetallic substrate: A strategy to maximize Pt utilization for fuel cells [J]. *Journal of the American Chemical Society*, 2014, 136: 9643–9649.
- [88] ALIPOUR MOGHADAM ESFAHANI R, EBRALIDZE I I, SPECCHIA S, EASTON E B. A fuel cell catalyst support based on doped titanium suboxides with enhanced conductivity, durability and fuel cell performance [J]. *Journal*

- of Materials Chemistry A, 2018, 6: 14805–14815.
- [89] ALIPOUR MOGHADAM ESFAHANI R, FRUEHWALD H M, LASCHUK N O, SULLIVAN M T, EGAN J G, EBRALIDZE I I, ZENKINA O V, EASTON E B. A highly durable N-enriched titanium nanotube suboxide fuel cell catalyst support [J]. Applied Catalysis B: Environmental, 2020, 263: 118272.
- [90] ALIPOUR MOGHADAM ESFAHANI R, EASTON E B. Exceptionally durable Pt/TOMS catalysts for fuel cells [J]. Applied Catalysis B: Environmental, 2020, 268: 118743.
- [91] ALIPOUR MOGHADAM ESFAHANI R, MOGHADDAM R B, EASTON E B. High performance Pt/Ti₃O₅Mo_{0.2}Si_{0.4} electrocatalyst with outstanding methanol oxidation activity [J]. Catalysis Science & Technology, 2019, 9: 4118–4124.
- [92] SHI Ru-yue, HUANG Ying, LI Miao-ran, ZHU Ying, HE Xue-xia, JIANG Rui-bin, LEI Zhi-bin, LIU Zong-huai, SUN Jie. Synthesis of Ti₄O₇/Ti₃O₅ dual-phase nanofibers with coherent interface for oxygen reduction reaction electrocatalysts [J]. Materials, 2020, 13: 3142.
- [93] SIREESHA P, SASIKUMAR R, CHEN S M, SU C C, RANGANATHAN P, RWEI S P. Carboxylic acid-functionalized multi-walled carbon nanotubes-polyindole/Ti₂O₃: A novel hybrid nanocomposite as highly efficient photo-anode for dye-sensitized solar cells (DSSCs) [J]. Applied Surface Science, 2017, 423: 147–153.
- [94] TOYODA M, YANO T, TRYBA B, MOZIA S, TSUMURA T, INAGAKI M. Preparation of carbon-coated Magnéli phases Ti_nO_{2n-1} and their photocatalytic activity under visible light [J]. Applied Catalysis B: Environmental, 2009, 88: 160–164.
- [95] ZHAO Xin, ZHANG Xiao-jing, ZHAO Bo-lin, JIA Fei, HAN Dong-xue, FAN Ying-ying, NIU Li, IVASKA A. A direct oxygen vacancy essential Z-scheme C@Ti₄O₇/g-C₃N₄ heterojunctions for visible-light degradation towards environmental dye pollutants [J]. Applied Surface Science, 2020, 525: 146486.
- [96] OU Gang, LI Zhi-wei, LI Dong-ke, CHENG Liang, LIU Zhuang, WU Hui. Photothermal therapy by using titanium oxide nanoparticles [J]. Nano Research, 2016, 9: 1236–1243.
- [97] STEM N, CHINAGLIA E F, DOS SANTOS FILHO S. G. Microscale meshes of Ti₃O₅ nano- and microfibers prepared via annealing of C-doped TiO₂ thin films [J]. Materials Science and Engineering: B, 2011, 176: 1190–1196.
- [98] STEM N, CHINAGLIA E D, DOS SANTOS FILHO S G. Ti₃O₅ nano- and microfibers prepared via annealing of C-doped TiO₂ thin films aiming at solar cell and photocatalysis applications [J]. ECS Transactions, 2011, 39: 347.
- [99] QI Wen-qian, DU Jun, PENG Yi-chao, WANG Ya-lin, XU Yong-qiang, LI Xiu-yun, ZHANG Kai, GONG Cheng, LUO Mei, PENG Hai-long. Self-induced preparation of Ti₃O₅ nanorods by chemical vapor deposition [J]. Vacuum, 2017, 143: 380–385.
- [100] YOSHIMATSU K, SAKATA O, OHTOMO A. Superconductivity in Ti₄O₇ and γ-Ti₃O₅ films [J]. Scientific Reports, 2017, 7: 12544.
- [101] FU Xian-kai, CHEN Wan-qi, HAO Xiao-wen, ZHANG Zhi-min, TANG Ruo-lan, YANG Bo, ZHAO Xiang, ZUO Liang. Preparing high purity λ-Ti₃O₅ and Li/λ-Ti₃O₅ as high-performance electromagnetic wave absorbers [J]. Journal of Materials Chemistry C, 2021, 9: 7976–7981.
- [102] LI Ya-hui, BAI Hua, ZHAI Jun-feng, YI Wen-cai, LI Jun-fang, YANG Hai-feng, XI Guang-cheng. Alternative to noble metal substrates: Metallic and plasmonic Ti₃O₅ hierarchical microspheres for surface enhanced Raman spectroscopy [J]. Analytical Chemistry, 2019, 91: 4496–4503.
- [103] DING Zhan-lin, WANG Hong, FENG Zhe, SUN Mei-qing. Synthesis of dual-phase Ti₃O₅/Ti₄O₇ nanofibers for efficient adsorption of SARS-CoV-2 [J]. Materials Letters, 2021, 300: 130167.

Ti₃O₅ 的合成、性能及应用研究进展

赵鹏飞^{1,2}, 李光石^{1,2}, 李文莉^{1,2}, 程鹏^{1,2}, 庞忠亚^{1,2}, 熊晓璐^{1,2}, 邹星礼^{1,2}, 许茜^{1,2}, 鲁雄刚^{1,2,3}

1. 上海大学 材料科学与工程学院, 上海 200444;

2. 上海大学 省部共建高品质特殊钢冶金与制备国家重点实验室&上海市钢铁冶金新技术开发应用重点实验室, 上海 200444;

3. 上海电机学院 材料学院, 上海 201306

摘要: 自 20 世纪 50 年代以来, 人们对 Ti₃O₅ 的晶体结构、物理、化学和相变性质进行了大量研究。不同晶体结构 Ti₃O₅(α、β、γ、δ 和 λ) 的性能各异, 特别是 λ 与 β 相之间独特的可逆相变现象吸引了越来越多的研究兴趣, 这也为 Ti₃O₅ 在能源和数据存储领域开辟了新的应用。近年来, Ti₃O₅ 材料在痕量检测、微波吸收和病毒吸附等方面的优异表现, 进一步拓宽了其应用领域。本文详细介绍不同晶体结构 Ti₃O₅ 的基本性质, 并对其制备方法和应用领域研究进展进行了系统的综述。

关键词: Ti₃O₅; 相变; 压力诱导; 数据存储; 催化剂载体

(Edited by Wei-ping CHEN)